Exploratory design of a compliant mechanism for a dynamic hand orthosis
Lessons learned

Bos, Ronald; Plettenburg, Dick; Herder, Just

DOI
10.1109/ICORR.2017.8009314

Publication date
2017

Document Version
Accepted author manuscript

Published in
Proceedings of the 2017 International Conference on Rehabilitation Robotics (ICORR)

Accepted Author Manuscript. Link to published article (IEEE): https://doi.org/10.1109/ICORR.2017.8009314

Exploratory design of a compliant mechanism for a dynamic hand orthosis: lessons learned

Ronald A. Bos[1], Dick H. Plettenburg[1], *Member, IEEE,* and Just L. Herder[2], *Member, IEEE*

***Abstract*— This study does not describe a success-story. Instead, it describes an exploratory process and the lessons learned while designing a compliant mechanism for a dynamic hand orthosis. Tools from engineering optimization and rapid prototyping techniques were used, with the goal to design a mechanism to compensate for hypertonic or contracted finger muscles. Results show that the mechanism did not reach its design constraints, mostly because it could not provide for the necessary stiffness and compliance at the same time. Hence, the presented approach is more suited for design problems with either lower forces or less displacement. It was concluded that physiological stiffness models are an important part when modeling hand orthoses. Moreover, further research on compliant mechanisms in dynamic hand orthoses should focus on the feasibility of implementing more complex three-dimensional shapes, i.e., compliant shell mechanisms.**

I. INTRODUCTION

The human hand is an amazingly complex organ capable of doing many different tasks. Unfortunately, there are many individuals that are impeded even in the most basic functionality, e.g., to open the hand and grasp objects, which hampers their ability to perform activities of daily living (ADLs). There can be numerous causes, but common examples include muscle hypertonia or contractures due to the consequences of stroke [1], [2] or other neuromuscular disorders [3], limiting the ability to fully extend the fingers. For these individuals dynamic hand orthoses can offer novel solutions, whose development is a fast-growing field of research [4], [5], [6], [7]. These solutions range from simple gloves that provide passive impairment compensation for daily assistance [8] to more advanced devices that monitor and aid movement of the fingers for home rehabilitation [9].

The design of the mechanism for a dynamic hand orthosis, however, remains a challenge. Especially for devices used during ADLs, the mechanism should be compact, lightweight, comfortable [10], and prevent hindrance of tactile feedback as much as possible. Even more, the axes of rotation should align with those of the human hand, which becomes difficult within the limited available space. Meeting all these criteria while still providing sufficient force output, is something that seems to be missing from a large list of existing devices [7]. Moreover, it appeared that there remain some less-used solutions whose feasibility can still be further explored. One example is the use of compliant mechanisms.

Instead of having mechanical joints, compliant mechanisms make use of elastic deformation in materials to create a force or displacement. It opens possibilities for creating monolithic structures, allowing for the design of compact, light-weight mechanisms, and easy use of rapid manufacturing methods. Moreover, they can admit minor misalignments by offering flexibility. A few examples exist where a dynamic hand orthosis uses a compliant mechanism. These range from using simple piano wires for passive support [11] to a more complex active device using multiple parallel leaf springs [12], [13]. Efficiencies for larger ranges of motion, however, are generally low and it is difficult to find the right combination of flexibility and stiffness [14].

The goal of this study is to explore the use of compliant mechanisms in a dynamic hand orthosis, using tools from engineering optimization. The main purpose of the mechanism is to facilitate active extension of the fingers in order to compensate for finger flexor hypertonia or muscle contractures, ultimately regaining hand function while performing ADLs. The exploratory nature serves as a method to examine the feasibility of the proposed mechanism, as well as to extract recommendations for future work.

II. DESIGN CRITERIA

This study uses tools from engineering optimization, which requires a well-defined set of design criteria as boundary conditions. A summary of the design criteria, along with their descriptions and implementations, is shown in Table I. They are described below in more detail.

A. Degrees of freedom (DOFs)

Using a simplified model of the hand, each finger has three joints that facilitate flexion/extension (FE) and abduction/adduction (AA) movements. The thumb facilitates two DOFs (FE and AA) in the carpometacarpal (CMC) joint, two (FE and AA) in the metacarpophalangeal (MCP) joint, and one (FE) in the interphalangeal (IP) joint. All other fingers have two DOFs (FE and AA) in each MCP joint, one (FE) in each proximal interphalangeal (PIP) joint, and one (FE) in each distal interphalangeal (DIP) joint. In total, this gives 21 DOFs and illustrates the diversity of possible movements.

This research is part of the Symbionics program, which is partially supported by the Dutch Technology foundation STW (#13524 and #13525), Hankamp Rehabilitation (Enschede, NL), Hocoma (Volketswil, CH), TMSi (Oldenzaal, NL), Moog (Nieuw Vennep, NL), FESTO (Delft, NL), and multiple Duchenne foundations (NL & USA). STW is part of the Netherlands Organization for Scientific Research (NWO), which is partly funded by the Ministry of Economic Affairs.

[1]Ronald A. Bos and Dick H. Plettenburg are with the Department of Biomechanical Engineering, Delft University of Technology, 2628 CD Delft, The Netherlands (r.a.bos@tudelft.nl, d.h.plettenburg@tudelft.nl)

[2]Just L. Herder is with the Department of Precision and Microsystems Engineering, Delft University of Technology, 2628 CD Delft, The Netherlands (j.l.herder@tudelft.nl)

TABLE I

LIST OF DESIGN CRITERIA FOR THE MECHANISM.

Criterium	Metric/description	Implementation
Degrees of freedom	Functional degrees of freedom [#]	1
Design domain	Cross-section [mm×mm]	26×17 mm
Finger stiffness	Rotational stiffness [Nm/rad]	≈0.5 Nm/rad per joint
	Flexion/extension angle [°]	60/0° per joint
Comfort	Resultant interaction force [N]	<5 N
	Unpredictable environment	Compliant mechanism

For functional use, the hand can be controlled by fewer DOFs. This occurs in the natural case through synergies and mechanical couplings between tendons and muscles, which often depend on the task to be executed and posture of the body. This phenomenon can be collectively termed as functional DOFs (fDOFs) [15], implying that not all DOFs need to be individually controlled for specific tasks [16].

For a dynamic hand orthosis, this means that not all DOFs of the impaired hand need to be individually assisted. In the presented case, merely being able to open the hand for grasping can be enough to regain hand function for ADLs, hence a single fDOF is considered sufficient. For further simplification, the mechanism is designed for a single finger, i.e., the index finger. The presented concept can be extended for multiple phalanges by using force-distributing mechanisms (e.g., whippletree).

B. Design domain

The dynamic hand orthosis should affect the hand's natural movements as little as possible. Consequently, occupying space in between the fingers should be avoided. Moreover, the mechanism should reside on the dorsal side of the hand for conservation of tactile feedback on the palmar side. For a single finger module, the height and width should be no more than the hand's thickness and finger breadth. This results in an available cross-section of 26×17 mm [17] above the finger, respectively. The longitudinal length is of lower impact, as long as the mechanism does not extend over the wrist or fingertip. Because linear actuators are commonly used in a hand orthosis [7], a linear force input is assumed to actuate the mechanism.

C. Finger stiffness

The mechanism should be able to carry the forces necessary to extend the fingers for individuals that suffer from hypertonic or contracted muscles. In [2], several subjects with a score of 1+ or 2 on the Modified Ashworth scale showed an order of magnitude of 0.2-0.8 Nm over roughly 60°, which translates into a rotational stiffness of around 0.5 Nm/rad per joint. An exact value, however, is almost impossible to determine because there exists a large variety in severity between individuals [18]. As an initial exploration of the presented concept which is able to accommodate hypertonic muscles with similar scores on the Ashworth scale, a stiffness of 0.5 Nm/rad with equilibrium position at 60° flexion was used for each joint during optimization.

D. Comfort

Comfort is an important aspect for a dynamic hand orthosis and may well determine its acceptance for daily use. Its interpretation in design criteria is difficult and can be considered subjective, but it is here defined in terms of interaction forces. Such forces occur during normal operation of the device, but also due to unpredictable forces or impacts which may occur while performing ADLs.

During normal operation, forces are applied on the hand on a regular basis and skin tissue damage may occur. A method of minimizing discomfort is to minimize the main contributor to skin tissue damage, which is internal strain in underlying tissue [19], but can also be measured as reduction in blood flow [20]. In [21], an 85% reduction in blood flow was reported for pressures ranging between 30–52 kPa applied at the palmar side of the fingers and for a duration of several minutes. Additionally, shear forces equally contribute to internal stresses and the resultant force which is applied should be considered [20]. In the case of active extension of the fingers, forces are most likely applied at the palmar side of the fingers and for shorter durations. Resultantly, forces can be in the higher range before damage occurs due to a thicker layer of skin [22] and short duration of loading [19]. When force is applied at a 1 cm^2 area on the finger, the maximum resultant force is defined as 5 N.

In practice, when considering a joint stiffness of 0.5 Nm/rad, a resultant force of 5 N would require a moment arm of >100 mm and is unrealistic. During the optimization process in this study, this constraint was therefore often altered to higher forces or even relaxed in order to find a more realistic design point.

Regardless of the operational forces, unpredictable forces or impacts can occur on the mechanism during ADLs. In this case, a compliant mechanism is beneficial and provides for a safe interaction between the user and device. Additionally, the lack of mechanical joints avoids frictional phenomena and the need for lubrication, but also allows for the design of monolithic, simplistic, and low-profile structures. More importantly, a compliant dynamic hand orthosis is robust against minor misalignments between the finger's joints and mechanism's joints. Such misalignments may cause numerous sources of discomfort to the user or even tissue damage, where pressure sores, joint dislocations or cartilage damage are among the possibilities depending on the user [23].

III. MECHANISM SYNTHESIS

A. Topology optimization

For initial inspiration on mass distribution of a compliant monolithic mechanism, a simplified topology optimization procedure was performed. The problem was reduced to a single-DOF mechanism actuated by a linear input force (F_{act}), where a desired output displacement at an angle

(u_{out}) is maximized around a fixation point (see Fig. 1(a)). The basis of the algorithm was formed by the 99-line structural optimization code presented in [24], which contains a simple finite element model (FEM) using Q4 elements in a predefined design domain. The design was varied by scaling the stiffness of the individual elements by an artificial density factor, ρ.

As the ideal compliant mechanism is a trade-off between stiffness and flexibility, the objective function was defined as a ratio between these terms [25, Eq. P4]:

$$\min_{\boldsymbol{\rho}} f(\boldsymbol{\rho}) = -\text{sign}(MSE)\frac{|MSE(\boldsymbol{\rho})|^m}{SE(\boldsymbol{\rho})^n} \quad (1)$$

Here, strain energy (SE) is the amount of elastic energy stored in the mechanism and serves as a measure of stiffness. Mutual strain energy (MSE) expresses a form of output deformation due to a virtual load and represents flexibility [26]. The parameters m and n were taken at 2 and 1, respectively. Sequential linear programming with move limits [27] was then used to update the design variables.

B. Shape optimization

Results from the topology optimization procedure were interpreted and translated into a general shape of the mechanism, which was parameterized by defining member lengths, angles and in-plane material thicknesses. The shape optimization procedure was then performed by using `fmincon`'s SQP algorithm in Matlab (version 2013b, Mathworks, Natick, MA, USA). The mechanism's performance for each iteration was evaluated through a nested FEM using ANSYS Mechanical APDL (version 15.0, ANSYS Inc., Canonsburg, PA, USA).

In this FEM, the members were modeled as BEAM188 elements with rectangular cross-sections and connected with MPC184 joint elements. The finger was included to represent the load and was modeled as a double pendulum with fixed base, having joints with a linear rotational stiffness of 0.5 Nm/rad and equilibrium points at a 60° flexion angle. Distance between the mechanism and finger skeleton was ensured by adding stiff beam elements whose lengths were equal to half the finger's thickness. Compliancy of skin tissue was neglected.

All elements had an out-of-plane thickness of 15 mm. The mechanism's material properties originated from available data on 3D-printed Nylon (Taulman 645 Nylon, $E \approx 0.2$ GPa, $\sigma_Y \approx 35$ MPa), whereas the finger's material was taken as relatively stiff compared to the mechanism ($E = 200$ GPa). The FEM was evaluated by subjecting it to a 40 N linear force at the mechanism and recording the maximum extension angles of the finger joints, reaction loads at the fixation points and maximum equivalent stress in the mechanism.

The optimizer's constraints originate from the remaining design criteria as previously described. Additional constraints were added that limited the material stresses and avoided infeasible configurations. All constraints were normalized to ensure equal contribution despite their differences in units.

The goal of the mechanism was to fully extend the fingers, hence the objective function was defined to minimize the difference between the obtained extension angle of the finger joints and full extension. This was formulated as:

$$\min_{\mathbf{x}} g(\mathbf{x}) = \left|\Delta\theta_{MCP}(\mathbf{x}) - \frac{\pi}{3}\right| + \left|\Delta\theta_{PIP}(\mathbf{x}) - \frac{\pi}{3}\right| \quad (2)$$

Here, $\mathbf{x}$ represents the collection of parameters to be optimized, $\Delta\theta_{MCP}$ the angular rotation of the MCP joint, and $\Delta\theta_{PIP}$ the angular rotation of the PIP joint. In order to account for the limited precision in rapid manufacturing methods, angles were rounded to the closest increment of 5 degrees and lengths were rounded to millimeters.

C. Prototyping

The mechanism was evaluated by fitting it onto a mock-up finger, where a linear actuation force of 0–40 N was applied using a test bench. Position was determined with a camera that took pictures at increments of 5 N applied force. Using image processing software, the joint angles were then determined by the angle between the vectors imposed by the joint centers. This was considered to be accurate with a +/- 1° variation. Actuation force was measured and monitored using a load cell (Zemic Inc, Santa Fe Springs, California).

The effects of possible misalignments were evaluated by fixating the mechanism at three different points on the phalanges of the mock-up finger and detecting changes in the joint angles. The same alterations were applied in the FEM analysis for comparison. These locations were defined at 1/4, 1/2, and 3/4 of the proximal phalange's length and were labeled PP1, PP2, and PP3. The same was done for the intermediate phalange and the locations were labeled IP1, IP2, and IP3 (see top left illustration in Fig. 4).

The compliant mechanism was made out of 3D-printed Nylon plastic (Taulman 645 Nylon). The mock-up finger was made with 3D-printed ABS plastic and was a modified from the open source InMoov hand [28]. Main modifications included the addition of fixation points for the mechanism, a rectangular cross-section in the phalanges for simplicity, mechanical stops at 90° flexion and 20° extension, and free-rotating pulleys with bearings for reduced friction. The finger stiffness was simulated with a tendon-like system. Specifically, a linear spring was connected to a string that was routed through the pulleys at each joint.

IV. RESULTS

A. Topology optimization

The result from the topology optimization procedure is shown in Fig. 1(a), accompanied by an interpretation of this result over multiple joints in Fig. 1(b). The interpretation follows from the following observations:

- The bottom layer of elements (pixels) can be replaced by the finger's skeletal structure.
- The mechanism consists of a smooth arching element and connects with the finger through flexure elements.

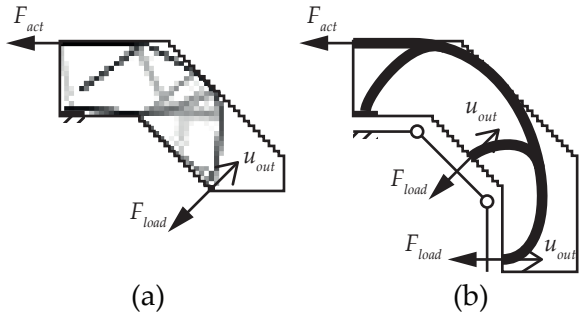

Fig. 1. (a) Result of the topology optimization procedure, indicating the input force (F_{act}), load force (F_{load}) and desired output displacement (u_{out}). Each pixel represents an element in de FEM, where darker pixels represent a higher local material stiffness and indicate a form of mass distribution. In (b), an interpretation of the result is illustrated across multiple joints.

- To prevent interference with the finger's knuckles, the flexure elements can be connected at the center of the phalanges.

B. Shape optimization

The resulting mechanism showed significant similarities with the compliant finger prosthesis from [29]. In this study, signs of buckling were observed in the flexure elements and were reduced by creating S-shaped flexures. This was also used in the parameterization of the mechanism for shape optimization, where the S-shape was characterized by two angles. In Fig. 2, a full parameterization of the mechanism is shown. The position of points A–O determined the mechanism's overall dimensions with respect to the finger, which were defined by its joints MCP–PIP–DIP. To create smooth shapes, the main arch of the mechanism was defined by creating a spline through points K–C–O–E–F–G, whereas the flexures were defined as two fillets between points H–I–J–K (and equivalently for L–M–N–O) with maximum radius. The line between A–K was defined as a straight line to ensure it remained parallel to the dorsal surface of the hand.

The locations of the fixation points (defined by l_{mH}, l_{pL}, and l_{iG}) were kept constant (30, 26.5, and 14 mm, respectively) and the parameter vector to be optimized was set at $\mathbf{x} = [\alpha_1, \alpha_2, \beta_1, \beta_2, \gamma, h_a, h_b, h_c, h_1, h_2, h_3]$. The resulting values are shown in Table II. In this shape and according to the FEM, the maximum equivalent stress was equal to 12.5 MPa and the final joint angles (negative indicating flexion) were predicted at -20° and -54° for the MCP and PIP joint, respectively. The resultant forces at the phalanges exceeded the constraints at approximately 7 N and 4 N at the proximal and intermediate phalange, respectively.

C. Prototyping

The resulting prototype of the mechanism with mock-up finger is shown in Fig. 3. The mechanism protruded a maximum of 22 mm in equilibrium position (flexed finger). During initial tests, the mechanism appeared not able to extend the fingers when the intended stiffness of 0.5 Nm/rad

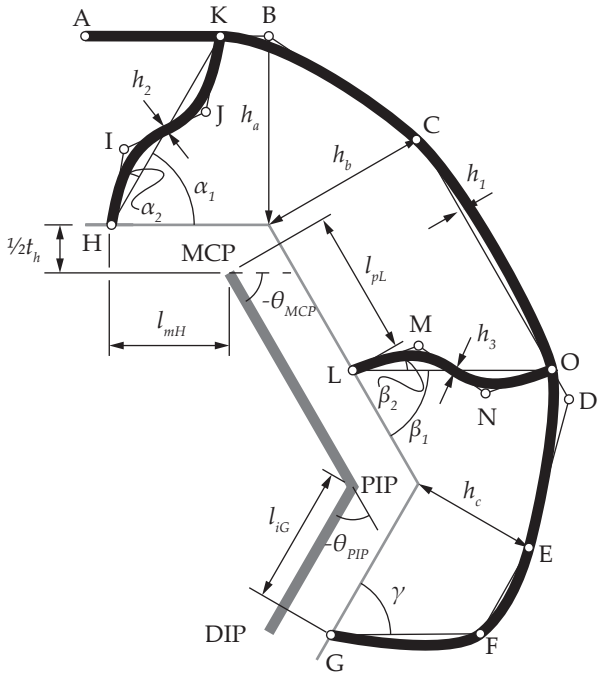

Fig. 2. Full parameterization of the mechanism shape, showing the finger skeleton (thick gray), skin surface (thin gray) and mechanism (thick black) outlines.

TABLE II

OPTIMIZED SHAPE FOR THE PARAMETERIZED MECHANISM.

PARAM.	ANGLE	PARAM.	LENGTH
α_1	40°	h_a	15 mm
α_2	-5°	h_b	22 mm
β_1	45°	h_c	22 mm
β_2	-35°	h_1	4 mm
γ	75°	h_2	5 mm
		h_3	4 mm

was applied. For this reason, a lower finger stiffness of approximately 0.2 Nm/rad was used and the model predictions were altered accordingly. The results from the FEM analysis and prototype measurements are shown in Fig. 4. In this graph, a range of curves due to imposed misalignments are also shown.

V. DISCUSSION

A. Finger stiffness

It is apparent from the results that the mechanism did not meet its design criteria and did not coincide with the model predictions. One of the major causes behind these differences was how the finger's joint stiffness was applied. In the FEM, each finger joint had an independent stiffness value, whereas the joints in the mock-up finger shared a stiffness through an underactuated tendon-like structure. This leads to a situation where an extension in the MCP joint would also increase the passive torque in the PIP joint. Because the mechanism had a more favorable moment arm around the MCP joint, it was more likely to extend and the PIP joint would remain flexed. A similar effect can be observed in the model results,

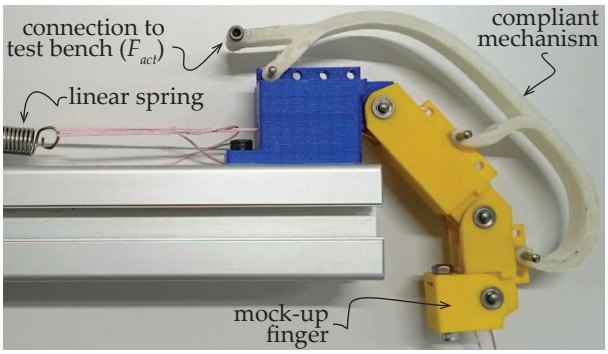

Fig. 3. Photo of the compliant mechanism made out of 3D-printed Nylon plastic, fixed onto a mock-up finger for testing purposes.

which only occurred after reducing the joint stiffness down to 0.2 Nm/rad (see Fig. 4).

These effects mostly demonstrate the mechanism's sensitivity to the finger's stiffness. Specifically, it shows that the stiffness model used during mechanism synthesis can have a large influence on the mechanism's performance, especially when it relies on an optimization procedure. It is therefore recommended to use models that better approach physiological behavior. For example in [30], [31], models are proposed with non-linear stiffness characteristics as well as dependencies on surrounding joint angles.

B. Mechanism shape

Due to a singularity around the PIP joint, the mechanism was not able to extend the PIP joint. This was caused by the direction of the forces on the phalanges and the mechanism's geometric shape. Depending on the PIP joint's angle, it would extend or flex as a result of the actuation force. Combined with the way how the joint stiffness was implemented in the mock-up finger (see previous subsection), this would cause the PIP joint to flex up to its mechanical stop (i.e., the 90° angle).

C. Material compliance

Similar to the model's predictions, the joint angle decreased when the fixations were moved to more proximal locations and increased when moved to distal locations. The size of the effect, however, was much larger in the measured results, indicating that the mechanism did not provide sufficient flexibility to cope with these changes. These differences are mostly attributed to the unpredictable mechanical properties of the material, as they are highly dependent on the 3D-printing process. In general, the material appeared to be stiffer than anticipated, which largely reduced motion around the Y-junctions at points K and O (see Fig. 2). Additionally, warped shapes along the vertical printing direction (out-of-plane thickness) was a common effect when printing the Nylon material. This would distort the second moment of inertia of the mechanism's cross-section and thus the resistance to bending.

These observations show that, when relying on rapid manufacturing methods, the actual behavior of the mechanism

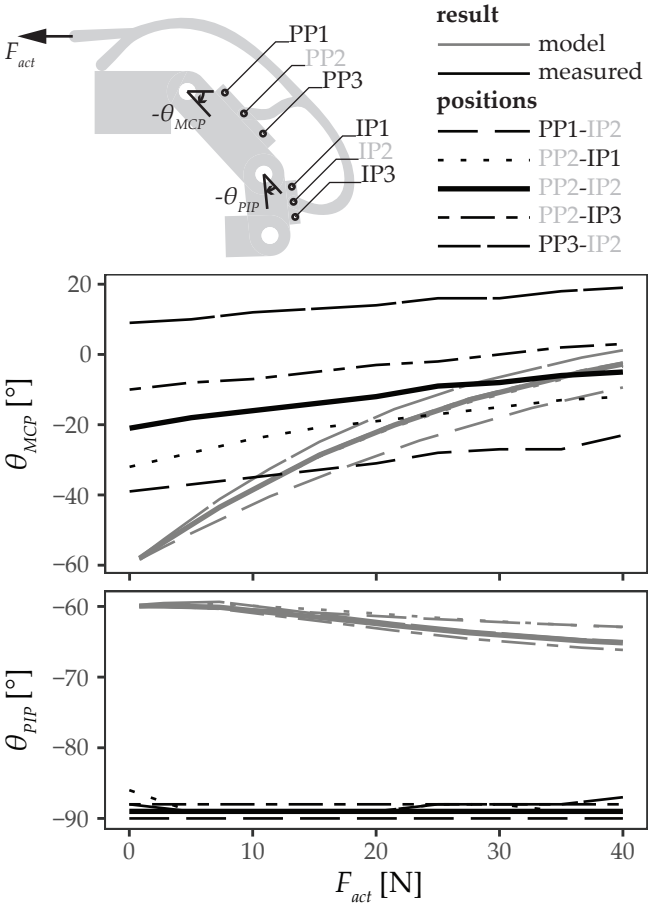

Fig. 4. Joint angles as a result of the input force F_{act}, comparing the model (gray) and measured (black) results. Please note the difference in vertical axis scaling. The top left illustration shows the outline shape of the mechanism on the mock-up finger, as well as the labels used in the legend. Misalignments are implemented by varying the fixation positions from a reference position PP2-IP2 (solid lines). Moving the fixations proximally (PP1 or IP1) decreases the flexion angle, moving them distally (PP3 or IP3) increases it.

can differ from the predictions. This implies that it would be more useful to investigate a range of design variations around an optimum, in order to investigate the prototype's sensitivities to these variations. Consequently, it can be recommended to perform a sensitivity analysis that includes the manufacturing process, instead of focusing on a singular result from an optimization procedure that may not be that optimal in practice.

The presented concept needed to withstand relatively high forces and large displacements, evidently requiring stiffness and compliance at the same time. Even though the 3D-printed Nylon plastic appeared very strong and flexible, a compliant mechanism in the presented shape would not be very suited for its original goal, i.e., to actively compensate contracted or hypertonic finger muscles. It may, however, be appropriate for applications with lower forces. For example, a thinner version may aid in minor force assistance during ADLs for individuals that only lack in muscular strength. Alternatively, the design problem can be expanded to a three-dimensional case. Cross-sectional shapes can then be

altered to better approach the desired stiffness profile and the abduction/adduction movement in the MCP joint can be included, resulting in a shell-like mechanism.

VI. CONCLUSION

The mechanism did not reach its design criteria. It was not able to accommodate the intended joint stiffness of 0.5 Nm/rad and even at a lower stiffness of the finger, it would only extend for 20°. Nevertheless, several lessons were learned from the process and can be useful as recommendation for future work.

Including the prototype of a 3D-printed compliant mechanism in the sensitivity analysis, would give a better view on the mechanism's behavior in practice and includes the rapid manufacturing process. This can be a more powerful tool than relying on a single optimal result. Moreover, it is important to implement a physiological joint stiffness model when modeling a hand orthosis. Especially when relying on optimization tools, the design becomes highly dependent on how the finger behaves. A compliant mechanism will also change shape depending on the forces applied, hence it has a large influence on the mechanism's outcome.

The original goal of the mechanism, i.e., to compensate for contracted or hypertonic finger muscles, did not appear to be compatible with the presented concept. At this scale, the necessary forces to be transmitted required the mechanism to be relatively stiff, but the necessary range of motion also required it to be compliant in the same direction. This approach may be better suited for other hand impairments or purposes that require either lower forces or less displacement. For future work, it is recommended to investigate the feasibility of compliant mechanisms with more complex three-dimensional shapes (shell mechanisms).

VII. ACKNOWLEDGMENT

The authors would like to thank Claudia J.W. Haarman for her support in making the 3D-printed components.

REFERENCES

[1] D. G. Kamper, R. L. Harvey, S. Suresh, and W. Z. Rymer, "Relative contributions of neural mechanisms versus muscle mechanics in promoting finger extension deficits following stroke," *Muscle Nerve*, vol. 28, no. 3, pp. 309–318, 2003.

[2] E. B. Brokaw, I. Black, R. J. Holley, and P. S. Lum, "Hand Spring Operated Movement Enhancer (HandSOME): a portable, passive hand exoskeleton for stroke rehabilitation," *IEEE Trans. Neural Syst. Rehab. Eng.*, vol. 19, no. 4, pp. 391–399, 2011.

[3] A. J. Skalsky and C. M. McDonald, "Prevention and Management of Limb Contractures in Neuromuscular Diseases," *Phys. Med. Rehabil. Clin. N. Am.*, vol. 23, no. 3, pp. 675–687, 2012.

[4] S. Balasubramanian, J. Klein, and E. Burdet, "Robot-assisted rehabilitation of hand function," *Curr. Opin. Neurol.*, vol. 23, no. 6, pp. 661–670, 2010.

[5] P. Heo, G. M. Gu, S. J. Lee, K. Rhee, and J. Kim, "Current hand exoskeleton technologies for rehabilitation and assistive engineering," *Int. J. Precis. Eng. Manuf.*, vol. 13, no. 5, pp. 807–824, 2012.

[6] P. Maciejasz, J. Eschweiler, K. Gerlach-Hahn, A. Jansen-Troy, and S. Leonhardt, "A survey on robotic devices for upper limb rehabilitation." *J. Neuroeng. Rehabil.*, vol. 11, no. 1, p. 3, 2014.

[7] R. A. Bos, C. J. Haarman, T. Stortelder, K. Nizamis, J. L. Herder, A. H. Stienen, and D. H. Plettenburg, "A structured overview of trends and technologies used in dynamic hand orthoses," *J. Neuroeng. Rehabil.*, vol. 13, no. 1, p. 62, 2016.

[8] Saebo, Inc., "SaeboGlove Brochure," https://www.saebo.com/wp-content/uploads/2016/01/SaeboGlove-Brochure.pdf, accessed 16 Jan 2017.

[9] S. Ates, C. J. W. Haarman, and A. H. A. Stienen, "SCRIPT passive orthosis: design of interactive hand and wrist exoskeleton for rehabilitation at home after stroke," *Auton. Robots*, pp. 1–13, 2016.

[10] B. Radder, A. Kottink, N. van der Vaart, D. Oosting, J. Buurke, S. Nijenhuis, G. Prange, and J. Rietman, "User-centred input for a wearable soft-robotic glove supporting hand function in daily life," in *2015 IEEE Int. Conf. Rehabil. Robot. (ICORR)*, Singapore, 2015, pp. 502–507.

[11] H. Watanabe, K. Ogata, T. Okabe, and T. Amano, "Hand orthosis for various finger impairments–the K U finger splint," *Prosthet. Orthot. Int.*, vol. 2, no. 2, pp. 95–100, 1978.

[12] J. Arata, K. Ohmoto, R. Gassert, O. Lambercy, H. Fujimoto, and I. Wada, "A new hand exoskeleton device for rehabilitation using a three-layered sliding spring mechanism," in *2013 IEEE Int. Conf. Robot. Autom. (ICRA)*, Karlsruhe, 2013, pp. 3902–3907.

[13] C. J. Nycz, T. Butzer, O. Lambercy, J. Arata, G. S. Fischer, and R. Gassert, "Design and Characterization of a Lightweight and Fully Portable Remote Actuation System for Use With a Hand Exoskeleton," *IEEE Robot. Autom. L.*, vol. 1, no. 2, pp. 976–983, 2016.

[14] E. Matheson and G. Brooker, "Augmented robotic device for EVA hand manoeuvres," *Acta Astronaut.*, vol. 81, no. 1, pp. 51–61, 2012.

[15] M. Santello, M. Flanders, and J. F. Soechting, "Postural hand synergies for tool use," *J. Neurosci.*, vol. 18, no. 23, pp. 10 105–10 115, 1998.

[16] M. Santello, M. Bianchi, M. Gabiccini, E. Ricciardi, G. Salvietti, D. Prattichizzo, M. Ernst, A. Moscatelli, H. Jörntell, A. M. Kappers, K. Kyriakopoulos, A. Albu-Schäffer, C. Castellini, and A. Bicchi, "Hand synergies: Integration of robotics and neuroscience for understanding the control of biological and artificial hands," *Phys. Life Rev.*, vol. 17, pp. 1–23, 2016.

[17] DINED anthropometric database, "Dutch adults, dined2004, 20–60 years," http://dined.io.tudelft.nl/en/database.

[18] D. G. Kamper and W. Z. Rymer, "Quantitative features of the stretch response of extrinsic finger muscles in hemiparetic stroke," *Muscle Nerve*, vol. 23, no. 6, pp. 954–961, 2000.

[19] C. Oomens, S. Loerakker, and D. Bader, "The importance of internal strain as opposed to interface pressure in the prevention of pressure related deep tissue injury," *J. Tissue Viability*, vol. 19, no. 2, pp. 35–42, 2010.

[20] M. Zhang, A. R. Turner-Smith, and V. C. Roberts, "The reaction of skin and soft tissue to shear forces applied externally to the skin surface," *Proc. Inst. Mech. Eng. H*, vol. 208, no. 4, pp. 217–222, 1994.

[21] L. Johansson, G. M. Hägg, and T. Fischer, "Skin blood flow in the human hand in relation to applied pressure," *Eur. J. Appl. Physiol.*, vol. 86, no. 5, pp. 394–400, 2002.

[22] L. Bennett, "Transferring load to flesh. Part III. Analysis of shear stress," *Bull. Prosthet. Res.*, vol. 10-17, pp. 38–51, 1972.

[23] A. Schiele and F. C. T. van der Helm, "Kinematic Design to Improve Ergonomics in Human Machine Interaction," *IEEE Trans. Neural Syst. Rehab. Eng.*, vol. 14, no. 4, pp. 456–469, 2006.

[24] O. Sigmund, "A 99 line topology optimization code written in matlab," *Struct. Multidiscipl. Optim.*, vol. 21, no. 2, pp. 120–127, 2001.

[25] A. Saxena and G. Ananthasuresh, "Topological synthesis of compliant mechanisms using the optimality criteria method," in *Proc. 7th AIAA/USAF/NASA/ISSMO Symp. Multidiscipl. Anal. Optim.*, 1998.

[26] L. L. Howell, *Compliant mechanisms*. John Wiley & Sons, 2001.

[27] O. Sigmund, "On the design of compliant mechanisms using topology optimization," *Mech. Struct. Mach.*, vol. 25, no. 4, pp. 493–524, 1997.

[28] Gael Langevin, "Hand robot InMoov," http://www.inmoov.fr/, accessed 16 Jan 2016.

[29] P. Steutel, "Design of a fully compliant under-actuated finger with a monolithic structure and distributed compliance," M.Sc. Thesis, Delft University of Technology, 2010.

[30] D. G. Kamper, T. George Hornby, and W. Z. Rymer, "Extrinsic flexor muscles generate concurrent flexion of all three finger joints," *J. Biomech.*, vol. 35, no. 12, pp. 1581–1589, 2002.

[31] A. D. Deshpande, N. Gialias, and Y. Matsuoka, "Contributions of intrinsic visco-elastic torques during planar index finger and wrist movements," *IEEE Trans. Biomed. Eng.*, vol. 59, no. 2, pp. 586–594, 2012.